
Article:
Celliers, P. M., Collins, G. W., Hicks, D. G. et al. (2004) Electronic conduction in shock-compressed water. Physics of Plasmas. L41-L44. ISSN: 1089-7674

https://doi.org/10.1063/1.1758944

Electronic conduction in shock-compressed water

P. M. Celliers,[1] G. W. Collins,[1] D. G. Hicks,[1] M. Koenig,[2] E. Henry,[2,3] A. Benuzzi-Mounaix,[2] D. Batani,[3] D. K. Bradley,[1] L. B. Da Silva,[1] R. J. Wallace,[1] S. J. Moon,[1] J. H. Eggert,[1] K. K. M. Lee,[4] L. R. Benedetti,[4] R. Jeanloz,[4] I. Masclet,[5] N. Dague,[5] B. Marchet,[5] M. Rabec Le Gloahec,[5] Ch. Reverdin,[5] J. Pasley,[6] O. Willi,[6] D. Neely,[7] and C. Danson[7]
[1]*Lawrence Livermore National Laboratory, Livermore, California 94551*
[2]*Laboratoire pour l'Utilisation des Lasers Intenses (LULI), Unité Mixte No. 7605, CNRS-CEA-Ecole Polytechnique-Université Pierre et Marie Curie, 91128 Palaiseau, France*
[3]*Dipartimento di Fisicà, G. Occhialini Universita degli Studi di Milano-Bicocca and INFM, 20126 Milan, Italy*
[4]*University of California, Berkeley, California 94720*
[5]*CEA/DAM Ile de France, 91680 Bruyères-le-Châtel, France*
[6]*Imperial College, London, United Kingdom*
[7]*Central Laser Facility, Rutherford Appleton Laboratory, Oxfordshire OX11 0QX, United Kingdom*

(Received 5 January 2004; accepted 8 April 2004; published online 25 June 2004)

The optical reflectance of a strong shock front in water increases continuously with pressure above 100 GPa and saturates at ~45% reflectance above 250 GPa. This is the first evidence of electronic conduction in high pressure water. In addition, the water Hugoniot equation of state up to 790 GPa (7.9 Mbar) is determined from shock velocity measurements made by detecting the Doppler shift of reflected light. From a fit to the reflectance data we find that an electronic mobility gap ~2.5 eV controls thermal activation of electronic carriers at pressures in the range of 100–150 GPa. This suggests that electronic conduction contributes significantly to the total conductivity along the Neptune isentrope above 150 GPa. © *2004 American Institute of Physics.*
[DOI: 10.1063/1.1758944]

Water is one of the most abundant molecules in the solar system, ubiquitous in biology, and a fundamental constituent of the giant planets Neptune and Uranus. In the center regions of the outer planets water exists at conditions distributed along an isentrope, at temperatures ranging from 2000 to 6000 K, and pressures ranging from 10 to 800 GPa.[1] Electrical conductivity at these conditions is important for understanding magnetic field generation in these planets.[2,3] Low temperature (295 K) water is insulating: the liquid at 0.1 MPa is an amorphous semiconductor with 6.5 eV gap energy;[4] solid phases are expected to remain insulating to pressures beyond 700 GPa with gap energies larger than 10 eV.[5] Shock compressed water becomes electrically conducting at rather low pressures: measurements of the dc conductivity, σ_{dc}, along the principal Hugoniot revealed an exponentially increasing trend up to 10 GPa,[6,7] followed by a much slower increase to a saturation level of $\sim 20\ (\Omega\ \mathrm{cm})^{-1}$ between 35 and 60 GPa.[8] This conductivity was attributed to dissociation into ionic species, possibly the bimolecular reaction $2H_2O \rightarrow OH^- + H_3O^+$. The result motivated a single shock Raman scattering study which revealed that the concentration of intermolecular hydrogen bonds begins to decrease at 12 GPa and vanishes at 26 GPa,[9] and inferred that the conduction mechanism may involve free protons, $H_2O \rightarrow OH^- + H^+$. Recent reverberating shock experiments achieved up to 180 GPa and 5400 K and found that σ_{dc} increased slowly to $200\ (\Omega\ \mathrm{cm})^{-1}$,[10,11] and remains ionic. Concurrent *ab initio* molecular dynamics investigations elucidated details of the ionic conduction mechanisms.[12,13] Under strong shock compression one expects thermally activated *electronic* carriers to begin to dominate, however, no theoretical or experimental work to date has focused on electronically conducting phases of high pressure, high temperature water.

In recent years large lasers have allowed access to pressures close to 1 TPa. Here we report on the equation of state (EOS) and optical reflectance of water compressed by a single strong shock wave spanning the pressure range of 100–790 GPa, a range for which no previous measurements exist. Several large lasers around the world were used, including the Phebus laser[14] and the LULI facility in France, the Omega laser in Rochester, NY,[15] and the Vulcan laser in the UK.[16] Previous dynamic measurements of the EOS of water have been carried out with explosive techniques[17–19] and with a two-stage light gas gun[8,20] to determine the principal Hugoniot accurately to about 100 GPa. A single datum at 1.4 TPa (Ref. 21) from an underground nuclear experiment has never been repeated. Within experimental uncertainty the new laser-shock data are consistent with existing data, and also with a tabular EOS from the SESAME database.[22,23] More important, we found a strong variation in optical reflectance along the Hugoniot: below 100 GPa water is opaque and low reflecting (a few %); above 100 GPa it transforms continuously into a metallic-like optical reflector that saturates at reflectivities near 40%–50%. The high reflectiv-

ity is the first unambiguous evidence of electronic conduction in high pressure water.

Cylindrical 6 mm diam stainless steel containers held samples of de-ionized, distilled 99.9% pure H_2O. One end of the container was sealed with a 500 μm thick sapphire window which allowed optical access to the water and water–aluminum interface. The opposite end of the container was sealed with a stepped Al plate (pusher) with the step facing the water. The Al pusher was fabricated from rolled 99.999% pure Al stock by diamond machining to produce step heights between 15 and 25 μm, measured to within 100 nm accuracy with a white light phase stepping interferometer. A thin polystyrene film, typically 15 μm overcoated with 100 nm of Al, was attached to the flat side of the aluminum plate and served as the ablator. Irradiation of the ablator with one or several smoothed[24,25] laser beams launched a strong shock which was transmitted into the Al plate and then into the water. Focal spot sizes 800 μm in diameter were used for some experiments and 400 μm for other experiments. For EOS measurements we used a 3.7 ns pulse to produce a steady shock wave, and for some reflectivity measurements we used a shorter 1 ns pulse to load the specimen impulsively and produce an attenuating shock wave to allow probing over a wide range of pressures.

A line-imaging velocity interferometer system for any reflector (VISAR)[26,27] recorded light reflected from the sample cell. This instrument works by reflecting an injection-seeded, Q-switched Nd:YAG laser probe beam from the rear of the target, and relaying an image of the target through a velocity interferometer onto a streak camera slit. For strong shocks in water (>100 GPa) the probe light was reflected directly from the shock front.[28] The Doppler shift of reflected light is manifested as a shift in fringe phase at the output of the velocity interferometer. In most cases we used two interferometers operating at wavelength $\lambda = 532$ nm with different velocity sensitivities to resolve fringe shift ambiguities. For some experiments we used a 1064 nm wavelength operating in one interferometer simultaneously with a 532 nm probe in the other interferometer.

An example recording (inset in Fig. 1) shows initially stationary fringes produced by the reflection of the probe beam from the Al pusher. The shock emerged first out of the thin Al step, later out of the thick step and was then transmitted to the water. The shock front in the water is reflecting and imparts a Doppler shift to the reflected probe, manifested as a fringe shift in the data recorded. We extracted three observables from the VISAR recordings for each shot: the shock velocity versus time, given by the fringe shifts; the shock reflectivity versus time, given by the reflected intensity; and the average shock velocity in the Al pusher, given by the break-out times from the top and bottom steps. Statistical uncertainties in the shock velocity determined from fringe shifts are typically 0.3%–1%. Typical uncertainties for the average shock speed in Al were 1.5%–3% and they dominate errors in EOS determination.

To determine EOS points we used the impedance-matching technique[29] which yields the pressure P and particle speed u_p at the interface between the Al pusher and the water sample. Used in this analysis are the measured shock

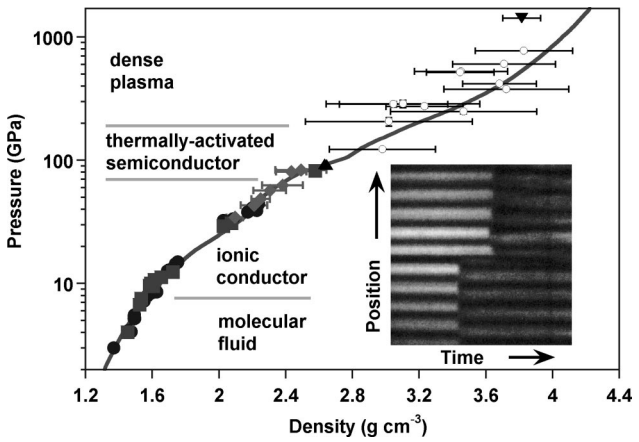

FIG. 1. Measurements of the principal Hugoniot of water: closed circles (Ref. 17), closed squares (Ref. 18), closed triangles (Ref. 19), closed diamonds (Ref. 8), inverted closed triangles (Ref. 21), open circles this work. The solid curve is the principal Hugoniot of water calculated from the SESAME database (Refs. 22 and 23). The inset shows typical data recorded that are described in the text.

velocities u_s for water and Al, and the known Hugoniot and release isentrope for the Al pusher.[22] The shock compression data shown in Fig. 1 include the early lower pressure experiments,[17,18] more recent higher pressure data,[8,19] and the single ultrahigh pressure datum.[21] Our laser shock data span the unexplored range between 100 and 800 GPa. The Hugoniot calculated from a tabulated EOS for water generated by Ree,[23] available in the SESAME database,[22] agrees well with the new data within experimental uncertainty. To compare these data with SESAME, a linear fit to the u_s vs u_p data determined here and the datum reported by Podurets *et al.*[21] was made. Over this limited pressure range, one in which no phase transitions are expected, a linear form for u_s vs u_p is quite good. This fit was converted to the $P-\rho$ plane using the Hugoniot relations. The difference in density between this fit and SESAME at 100, 500, and 1000 GPa is 0%, 6%, and 4%, respectively. While these values are within the density uncertainties estimated in this work, the data are systematically shifted toward lower density compared to SESAME at pressures between 200 and 1400 GPa.

We measured the reflectance of the shock by comparing the probe intensity reflected from the shock to that from the bare Al surface which has a known reflectivity of 0.85 ± 0.05. These data are shown in Fig. 2. The systematic error incurred in this process could be up to 10%. Relative uncertainties in the reflectance are typically about 20%. For some experiments we observed that an attenuating shock in the sample produces a continuous record of reflectance as a function of the shock velocity; the attenuating shock was generated by driving the Al pusher with a short (1 ns) high pressure pulse, which allowed rarefaction to overtake the shock propagating in the Al pusher before it reached the sample. In this case simultaneous recording of the Doppler shift (fringe phase) and intensity allowed us to extract shock reflectance over a wide range of shock states. Since the shock was not steady the compressed material behind it contained spatial density gradients along the propagation direction; however the gradient scale length is much larger than

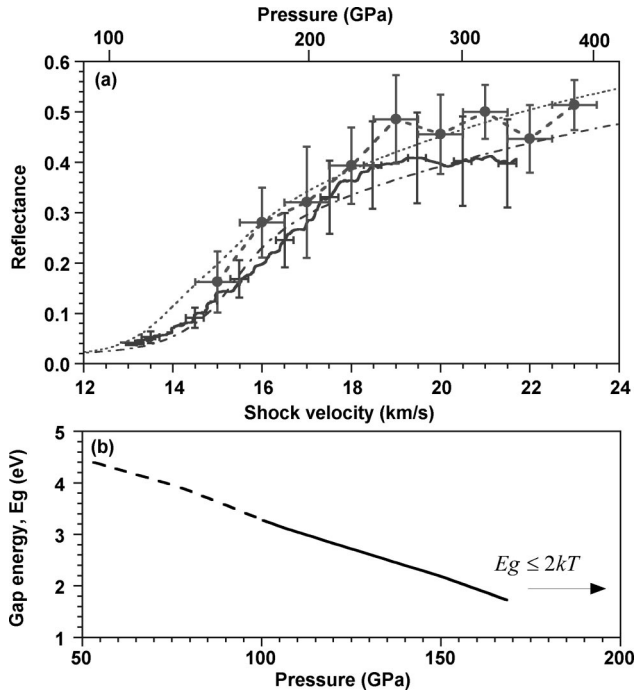

FIG. 2. (a) Optical reflectance of the shock front as a function of the shock velocity and pressure along the principal Hugoniot at 532 nm (solid line with error bars) and at 1064 nm (dashed line with closed cirles and error bars). Fits to these data are shown for 532 nm (chain-dashed) and 1064 nm (dotted) curve for the semiconductor model described in the text. (b) Variation of the mobility gap energy along the Hugoniot, extracted from the reflectance curve fits. Below 100 GPa (dashed) the reflectance is low and there are no data with which to constrain the fit. Above ~170 GPa the curve is terminated where $E_g/2kT \leqslant 1$.

the skin depth of the reflected light, ~0.1 μm.

Temperatures (T) predicted from the SESAME EOS model agree to better than 10% with measurements at lower pressures,[20,30] so we expect the EOS model to be reasonably accurate. For 100 GPa$< P <$300 GPa the model predicts 7000 K$\leqslant T \leqslant$30 000 K, and compression $2.7 < \rho/\rho_0 < 3.5$. While one would expect some increase in reflectivity from a compression-driven increase in the refractive index,[30] this can account for at most about 4% reflectivity assuming that the fluid remains an insulator; this is much smaller than the observed saturation levels of 40%–50%. Therefore we attribute rapidly increasing reflectivity above 100 GPa to free carriers generated by thermal activation across a mobility gap.

To model the reflectivity we use a standard semiconductor formalism to estimate the carrier density,[31] $N_e = 2(m_e kT/2\pi\hbar^2)^{3/2} F(-E_g/2kT)$ where m_e is the effective mass, k is the Boltzmann constant, E_g is the mobility gap energy in the electronic density of states, and $F(\eta) = (2/\sqrt{\pi}) \int_0^\infty \sqrt{x}/[1+\exp(x-\eta)]dx$. The dielectric function is given by a Drude-like expression, $\epsilon = \epsilon_b - \omega_p^2/\omega^2(1 + i/\omega\tau)$, where ϵ_b is the contribution due to bound electrons, ω is the angular frequency of the probe beam, and τ is the electron relaxation time. The plasma frequency is $\omega_p^2 = 4\pi N_e e^2/m^*$, where e is the electron charge, and $m^* = m_e/2$ is the reduced mass. Consistent with the treatment of intrinsic semiconductors, the chemical potential is placed midway within the gap and the mass of the holes and electrons is assumed equal. The relaxation time is taken as $\tau = \gamma\tau_{\min}$ where $\tau_{\min} = l/v_e$ is the minimum scattering time (Ioffe–Regel limit[32]) and $\gamma \gtrsim 1$. Here $l = 2(3/4\pi N_i)^{1/3}$ is the interparticle distance, N_i is the total number of particles per unit volume (H_2O or H_3O^+ and OH^- and others) and v_e is the electron velocity computed by integrating over the Fermi distribution at a given temperature. Estimating the bound electron contribution ϵ_b is problematic because of the disruption of chemical bonding that occurs above 25 GPa.[9,12,13] In the absence of data or models we used $\epsilon_b = 1$. (Variations in ϵ_b affect the calculated reflectivity mainly below 100 GPa, where we have no data with which to constrain a fit.) We calculate the reflectivity from the complex index of refraction, $n = \sqrt{\epsilon}$, and the Fresnel formula, $R = |(n-n_0)/(n+n_0)|^2$, where $n_0 = 1.33$ is the index of unshocked water.

Using this model to calculate the reflectivity we have fit the observed reflectance along the compression curve assuming a linear variation of E_g along the Hugoniot with respect to the density and temperature: E_g (eV) $= 6.5 - a(\rho/\rho_0 - 1) - b(T/T_0 - 1)$, with $\rho_0 = 0.998$ g cm^{-3} and $T_0 = 295$ K. This form is consistent with the known gap energy of 6.5 eV at the initial state,[4] and takes into account an expected variation in density and temperature of the gap energy.[12] The three-parameter best fit, $a = 1.32$, $b = 0.043$ and $\gamma = 1.05$, produces a varying gap energy ranging from 3.3 to 2 eV within the range of 100–150 GPa, respectively.[33] The variation of E_g along the Hugoniot is shown in Fig. 2(b). The predicted reflectivities compare well with the observations at both 532 and 1064 nm. Increasing E_g tends to shift the predicted rising edge of the reflectance toward higher velocities (higher P and T), while the collisionality factor γ controls the reflectivity in the saturation limit at high P and T (larger γ leads to larger conductivity and higher reflectivity). The relaxation time is close to the Ioffe–Regel limit[32] (i.e., $\gamma \sim 1$), indicative of strong scattering. This behavior has been found in shock compressed D_2,[34] as well as in LiF and Al_2O_3.[35] When $E_g/2kT \leqslant 1$ the gap is effectively closed through temperature smearing of the Fermi distribution, and the fluid is better characterized as a dense plasma. For shock-compressed water this transition occurs for $P \geqslant 170$ GPa, and $T \geqslant 15\,000$ K.

While this simple model does match the initial increase in shock reflectance well, it does not reproduce the reflectance saturation observed in the data. The observed saturation can be accounted for by limiting the carrier density near 10^{22} cm^{-3} at about 2300 K (250 GPa). This amounts to about 1 in 10 initial molecules contributing a free carrier, suggesting that even at these extreme temperatures and pressures, the chemistry is quite complex.

It is interesting to compare electrical conductivities estimated from this model with earlier measurements of σ_{dc},[8,10,11] which all point to an electronically insulating ionic conduction mechanism; in particular, observations of the galvanic potential between dissimilar electrodes[10] confirmed this. Using the reflectivity fit to determine $N_e(E_g)$, we estimate the electronic contribution to the dc conductivity using a Drude model, $\sigma_e = N_e e^2 \gamma \tau_{\min}/m^*$. Figure 3 shows a comparison of the estimated σ_e that corresponds to the states

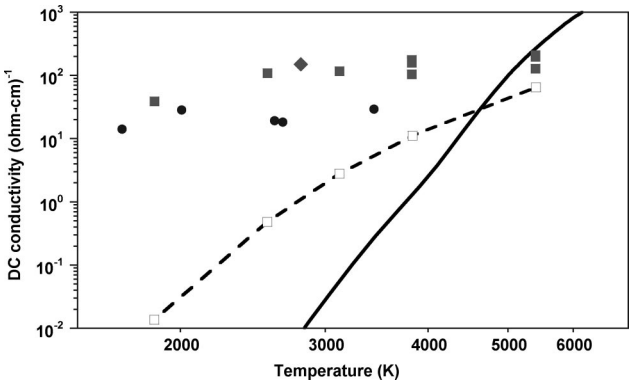

FIG. 3. Comparison of σ_{dc} from Ref. 8 (closed circles), from Ref. 11 (closed squares), from Ref. 10 (closed diamond) and σ_e (open squares and dashed curve) as a function of that temperature. Each of the open squares was computed for the states observed in Ref. 11 (closed squares at same T). The solid curve shows the estimated σ_e for water at states distributed along the Neptune isentrope.

observed by Chau *et al.* In this comparison we find that $\sigma_e \ll \sigma_{\mathrm{dc}}$ except at the highest pressure observed, 180 GPa, where $\sigma_e/\sigma_{\mathrm{dc}}$ is about 1/3. Thus E_g is high enough to prevent significant electronic conduction for the sample conditions observed in Refs. 10 and 11 consistent with the conclusions of those studies.

Above 5000 K (where the Chau *et al.* measurements stop) we estimate that σ_e will begin to dominate. This has implications for conductivity estimates in the interior of Neptune and Uranus. We have computed σ_e along the Neptune isentrope, also shown in Fig. 3, and find that σ_e contributes at least as much as the ionic contribution at temperatures above 5000 K. This may have significant bearing on planetary models that rely on conductivity data to understand generation of the magnetic field. Temperatures between 4500 and 6000 K correspond to a broad range of pressures, from 150 to 800 GPa along this isentrope; furthermore, details of this isentrope are model dependent and rather uncertain. Since the thermally activated nature of σ_e depends exponentially on both T and E_g, the electronic conductivity will depend strongly on precise details of how both E_g and T vary along the isentrope. By comparing a variety of models that match the reflectance data, we estimate that the electron conductivity model presented here is accurate to within about a factor 4 at temperatures between 1000 and 23000 K and pressures between 15 and 250 GPa.

The authors thank the operations staff at the Phebus, LULI, Omega and Vulcan facilities, and W. Unites for their effort during these experiments.

This work was performed under the auspices of the U.S. DOE by Lawrence Livermore National Laboratory (LLNL) under Contract No. W-7405-ENG-48, and also supported under EU Training and Mobility Research Contract Nos. ERBFMGECT 950016 (Phebus) and ERBFMGE-CT95-0044 (LULI), as well as LULI ACCESS HPRI-1999-CT 00052.

[1] W. B. Hubbard, Science **275**, 1279 (1997).
[2] W. J. Nellis *et al.*, Science **240**, 779 (1988).
[3] N. F. Ness *et al.*, Science **246**, 1473 (1989).
[4] F. Williams, S. Varma, and S. Hillenius, J. Chem. Phys. **64**, 1549 (1976).
[5] M. Benoit *et al.*, Phys. Rev. Lett. **76**, 2934 (1996).
[6] H. David and S. Hamann, Trans. Faraday Soc. **55**, 72 (1959).
[7] S. Hamann and M. Linton, Trans. Faraday Soc. **62**, 2234 (1966).
[8] A. C. Mitchell and W. J. Nellis, J. Chem. Phys. **76**, 6273 (1982).
[9] N. C. Holmes *et al.*, Phys. Rev. Lett. **55**, 2433 (1985).
[10] V. V. Yakushev *et al.*, JETP **90**, 617 (2000).
[11] R. Chau *et al.*, J. Chem. Phys. **114**, 1361 (2001), temperatures listed here are incorrect, Fig. 3 uses correct values.
[12] C. Cavazzoni *et al.*, Science **283**, (1999).
[13] E. Schwegler *et al.*, Phys. Rev. Lett. **87**, 265501 (2001).
[14] G. Thiell *et al.*, Laser Part. Beams **6**, 93 (1988).
[15] T. R. Boehly *et al.*, Opt. Commun. **133**, 495 (1997).
[16] I. N. Ross *et al.*, IEEE J. Quantum Electron. **QE-17**, 1653 (1981).
[17] J. M. Walsh and M. H. Rice, J. Chem. Phys. **26**, 815 (1957).
[18] L. V. Al'tshuler, A. A. Bakanova, and R. F. Trunin, Sov. Phys. Dokl. **3**, 761 (1959).
[19] L. P. Volkov *et al.*, JETP Lett. **31**, 513 (1980).
[20] G. A. Lyzenga, T. J. Ahrens, W. J. Nellis, and A. C. Mitchell, J. Chem. Phys. **76**, 6282 (1982).
[21] M. A. Podurets *et al.*, Sov. Phys. JETP **35**, 375 (1972).
[22] See National Technical Information Service Document No. DE94-011699. (J. D. Johnson, SESAME Tables, 1994). Copies may be ordered from the National Technical Information Service, Springfield, VA 22161. For the aluminum standard we used SESAME table 3719. The water table used here was SESAME table 7150.
[23] F. H. Ree, J. Chem. Phys. **12**, 6287 (1982).
[24] T. H. Bett *et al.*, Appl. Opt. **34**, 4025 (1995).
[25] S. N. Dixit *et al.*, Opt. Lett. **19**, 417 (1994).
[26] L. Barker and R. Hollenbach, J. Appl. Phys. **43**, 4669 (1972).
[27] P. M. Celliers *et al.*, Appl. Phys. Lett. **73**, 1320 (1998).
[28] To check this we tracked propagation of the shock across a gap formed by placing a quartz plate a known distance from the lower Al step. The gap distance found by integrating the VISAR signal between breakout and impact matched the known gap distance to within measurement accuracy ($\sim 1\%$).
[29] W. J. Nellis and A. C. Mitchell, J. Chem. Phys. **73**, 6137 (1980).
[30] S. Kormer, Sov. Phys. Usp. **11**, 229 (1968).
[31] C. Kittel and H. Kroemer, *Thermal Physics*, 2nd ed. (Freeman, San Francisco, 1980).
[32] A. Ioffe and A. Regel, Prog. Semicond. **4**, 237 (1969).
[33] Fits to $E_g = \mathrm{const}$, and $E_g = 6.5 - a(\rho/\rho_0 - 1)$ result in $\gamma \sim 1.4$ and produce very similar reflectivity curves. The reflectance data do not provide a strong constraint on the functional dependence of E_g, and all fits lead to $E_g \sim 2-3$ eV and $\gamma \sim 1$ in the pressure range of 100–200 GPa.
[34] P. M. Celliers *et al.*, Phys. Rev. Lett. **84**, 5564 (2000).
[35] D. Hicks *et al.*, Phys. Rev. Lett. **91**, 035502 (2003).